Int. J. Electrochem. Sci., 7 **(2012)** 3265 - 3273

International Journal of
ELECTROCHEMICAL
SCIENCE
www.electrochemsci.org

Formation of Hierarchical PtZn Alloy Films under Highly Cathodic Polarization of Pure Pt in a Dilute $ZnSO_4$ Solution and Their Electrocatalytic Applications

Yuan Yao, Shili Xu, Yue Xia, Yingchang Yang, Jun Liu, Zelin Li, Wei Huang[*]

Key Laboratory of Chemical Biology and Traditional Chinese Medicine Research (Ministry of Education of China), College of Chemistry and Chemical Engineering, Hunan Normal University, Changsha 410081, China
[*]E-mail: hjhw9513@163.com

Received: 26 February 2012 / *Accepted:* 14 March 2012 / *Published:* 1 April 2012

In this paper, hierarchical and high-rough PtZn alloy films were cathodically fabricated from a smooth Pt substrate in an alkaline aqueous solution of low $ZnSO_4$ concentration at a moderate temperature of 40 °C. Subsequently, the Pt/Zn atomic ratios for the films were regulated by dissolution of bulk Zn and partial dealloying of alloyed Zn in a H_2SO_4 solution under lower and higher anodic potentials, respectively. The films were characterized by scanning electron microscopy (SEM), energy dispersive X-ray spectroscopy (EDS) and X-ray photoelectron spectroscopy (XPS). The film formation might be closely related to processes including Zn electrodeposition, PtZn alloying, hydrogen evolution and cathodic corrosion of Pt under highly cathodic polarization. The as-prepared films exhibit better electrocatalytic activities toward the oxidation of formic acid and methanol, as compared with smooth Pt and PtZn films prepared under less cathodic polarization (without hydrogen evolution).

Keywords: Hierarchical films, PtZn alloys, highly cathodic polarization, cathodic corrosion, electrocatalysis

1. INTRODUCTION

Pt metal is a key catalyst for the electrooxidation of small organic molecules [1-2]. Addition of some foreign metals, such as Au [3], Ru [4], Pb [5], Rh [6], Co [7], Cu [8], Mo [9], Ni [10] and Sn [11], can effectively improve the electrocatalytic activity and lower the cost. Zn is a relatively cheap element, and the addition of it into Pt would lead to the formation of PtZn alloys and induces the redistribution of charge around Pt and Zn, resulting in significant changes in its properties [12]. In previous studies, vaporization [13] methods are often used to fabricate PtZn alloys. Such physical methods are carried out in a furnace without air exposure. Electrodeposition is a good alternative to prepare PtZn catalysts due to several advantages such as easy control and inexpensive equipments [14-18]. The researches related are usually carried out in non-aqueous ionic liquid systems [14-15] at elevated temperature, or in aqueous systems before the potential range of strong hydrogen evolution [16-18]. Up to now, as far as we know, less attention is paid to the electrodeposition of nanostructured PtZn films under highly cathodic polarization involving hydrogen evolution at mild temperature.

Here, we report the cathodic fabrication of hierarchical PtZn alloy films from pure Pt under highly polarization in an alkaline aqueous solution of low $ZnSO_4$ concentration at 40 ^oC. The electrocatalytic activities of the prepared PtZn alloy films toward the oxidation of formic acid and methanol are also presented.

2. EXPERIMENTAL PART

Electrochemical experiments were carried out in a conventional H-type glass cell with a CHI 660C electrochemical station (Chenhua Instruments, Shanghai, China). A Pt disk (1 mm in diameter, purity ≥ 99.99%), a large Pt foil, and a saturated mercurous sulfate electrode (SMSE) were employed as the working, counter and reference electrode, respectively. Prior to use the Pt disk was polished with 1200 grit Carbimet paper, followed by rinsing in Millipore water with ultrasonic waves. Then, the Pt electrode was electrochemically cleaned in 0.5 mol/L H_2SO_4 by cyclic voltammetry (CV) at 100 mV s^{-1} between –0.7 and 0.8 V until a stable voltammogram was observed. The clean Pt electrode was treated under highly cathodic polarization with a potential of –6 V (violent hydrogen evolution) for different time (1000 s typically) in 1 mmol/L $ZnSO_4$ + 2 mol/L NaOH at 40 °C. Subsequent anodic treatment (dissolution of bulk Zn) was conducted at a low potential of –0.4 V in 0.5 mol/L H_2SO_4 for 200 s to get hierarchical PtZn films with high Zn content (PtZn-1). To further decrease the Zn content, an alternative treatment was performed in the same solution but at a higher anodic potential of 0.4 V followed by repeated potential sweep (–0.7 ~ 0.8 V), and the as-prepared films were denoted as PtZn-2. For comparison, a third PtZn film (PtZn-3) was also prepared under less cathodic polarization with a potential of −1.55 V (no hydrogen evolution) for 1000 s in 0.1 mol/L $ZnSO_4$ and then treated at –0.4 V in 0.5 mol/L H_2SO_4 for 200 s.

The electrocatalytical activities of these films were tested in 0.5 mol/L CH_3OH + 0.5 mol/L H_2SO_4 or 0.5 mol/L HCOOH + 0.5 mol/L H_2SO_4. Unless specified otherwise, the current density was normalized to the electrochemically active surface area of each electrode using a hydrogen ad/desorption charge of 210 μC cm^{-2} for Pt in 0.5 mol/L H_2SO_4 [19]. This charge density is also used to calculate the film roughness (R).

The morphologies of the PtZn films were characterized by a field emission scanning electron microscope (FESEM, Nova NanoSEM 230). The surface compositions of the film electrodes were analyzed with an ESCA-Lab250 X-ray photoelectron spectroscopy (XPS) and the energy dispersive spectrometer (EDS). All solutions were freshly prepared with Millipore water and analytical grade chemicals.

3. RESULTS AND DISCUSSION

Fig. 1a shows the first potential sweep in 0.5 mol/L H_2SO_4 for the Pt electrode treated at –6 V in 2 mol/L NaOH containing 1 mmol/L $ZnSO_4$. In this curve, two oxidation peaks appeared obviously at –0.4 V and 0.29 V, which were related with the stripping of bulk and alloyed Zn, respectively [20]. According that, the PtZn films with lower and higher content of Pt (PtZn-1 and PtZn-2) should be formed when the newly-cathodized Pt electrode was anodized in H_2SO_4 solution at lower (–0.4 V) and higher (0.4 V) anodic potentials, respectively. The CV curve for the PtZn-2 film is shown in Fig. 1b. Noticeably, the behavior is similar to the pure Pt (Fig. 1d), indicating a high Pt content in the film. For comparison, the CV behavior of the PtZn-3 film prepared at a less cathodic polarization potential (–1.55 V) without hydrogen evolution in 0.1 mol/L $ZnSO_4$ is also exhibited as Fig. 1c. Note that bulk deposition of Zn commences at about –1.5 V [21], which can also be seen from the inset of Fig. 1. Obviously, the current for hydrogen ad/desorption at the PtZn-2 film is much larger than that of the PtZn-3 film and the smooth Pt, indicating that the surface of the PtZn-2 film is highly rough (R=112). This will be further confirmed by SEM characterization in the next part. Therefore, the condition under highly cathodic polarization accompanying hydrogen evolution is necessary in the fabrication of high-rough hierarchical PtZn film.

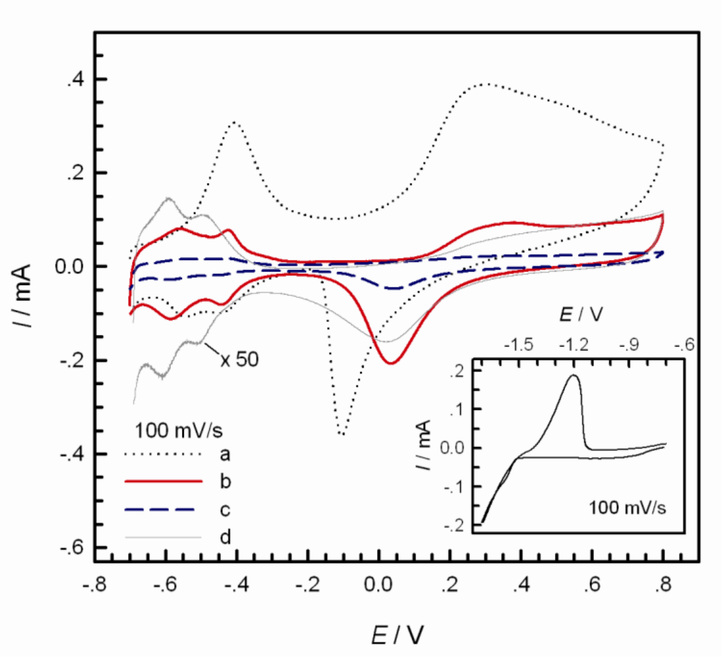

Figure 1. The (a) first and (b-d) stable CVs in 0.5 mol/L H_2SO_4 on the (d) smooth Pt and (b, c) PtZn films obtained by cathodically polarizing the Pt electrode at 40 °C for 1000 s (b) at –6 V in 1 mmol/L $ZnSO_4$ + 2 mol/L NaOH and (c) at –1.55 V in 0.1 mol/L $ZnSO_4$. The inset shows the CV for the smooth Pt in 0.1 mol/L $ZnSO_4$.

Fig. 2 shows the morphology of the PtZn-1 and PtZn-2 films. As seen from Fig. 2(a) and (c), no obvious difference exists between them. Both the surfaces exhibit a two-layer hierarchical characteristic. The cover layer looks loose, wrinkled and curly and is cracked into micron-area flakes.

The thickness of these flakes is estimated within 500 nm (Fig. 2(b) and (d)). On the other hand, the underneath layer displays nanoporous structure (Fig. 2(b) and (d)). Thus, the films with such a hierarchical nanostructure possess high surface area.

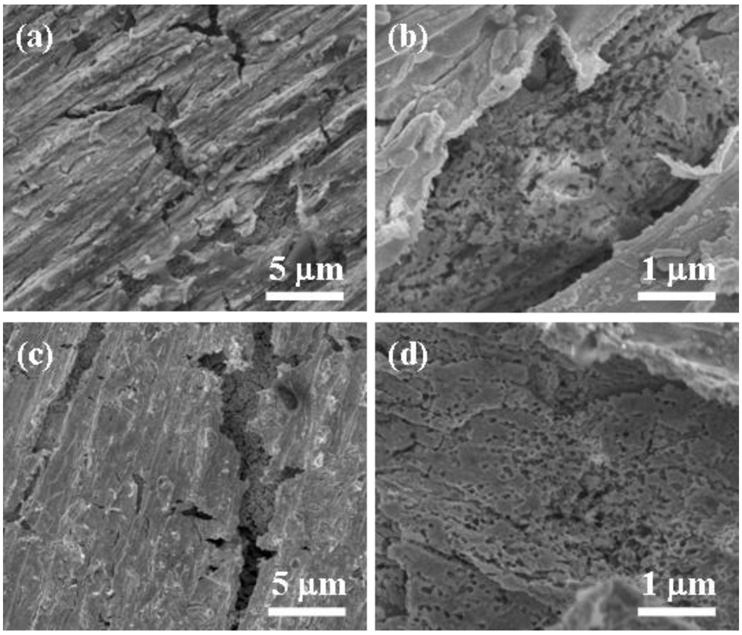

Figure 2. FESEM images with different enlargements of the hierarchical (a-b) PtZn-1 and (c-d) PtZn-2 films.

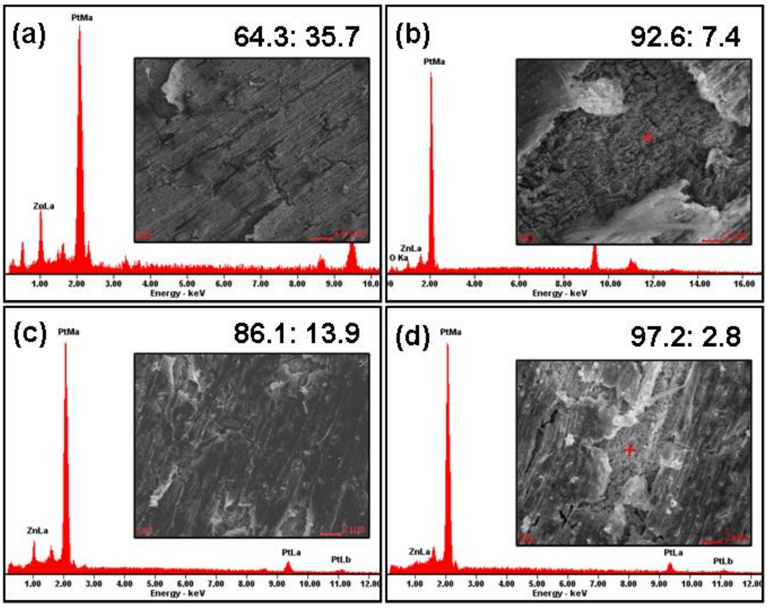

Figure 3. EDS spectra for the (a, b) PtZn-1 and (c, d) PtZn-2 films taken on (a, c) the cover layer and (b, d) the underneath porous layer. The insets are the corresponding SEM images and the symbols "+" in 3(b) and 3(d) show the acquisition points. The Pt/Zn atomic ratio is shown at the top right corner of each figure.

The EDS spectra of the hierarchical PtZn films collected on different area are displayed in Fig. 3. On the whole, the Pt content in them is predominant. Noticeably, the Zn content for the PtZn-1 film (35.7%, Fig. 3(a)) is more than twice as high as that for the PtZn-2 film (13.9%, Fig. 3(c)) although the two films own similar surface. Obviously, the anodic dissolution at higher potential further reduces the content of Zn comparing to that at lower potential, but it is uneasy to remove Zn completely from PtZn alloys at 0.4 V. This phenomenon was also observed previously for PtZn alloys treated in hot concentrated nitric acid or hot concentrated hydrochloric acid [18]. In acidic electrochemical environments, Zn can not be removed completely in short time unless PtZn alloy was treated at 1.25 V (vs. RHE) for at least 2.5 h [16]. As seen in Fig. 3(b) and (d), the Zn contents in the underneath nanoporous layer of the two films are reduced to 7.4% and 2.8%, respectively, which are lower markedly than those on the large-area surfaces (Fig. 3(a) and (c)). There are two possible explanations for the difference of Zn content between the cover and underneath layer. One is that the alloying extent for the inner layer is lower than the cover layer. The other is that more signal of Pt substrate was taken for the porous layer than for the cover layer, considering that the detection depth of EDS is up to several microns [22] which is probably larger than the PtZn film thickness.

XPS analysis was employed to characterize the surface compositions and properties of PtZn-1 alloy films prepared at – 6 V for 100 s and 1000 s (Fig. 4). It can be seen from Fig. 4 that the spectra of Pt 4f (a) and Zn 2p (b) relating to the two samples are basically the same. The Pt $4f_{7/2}$ and Zn $2p_{1/2}$ core level binding energies and the Pt:Zn ratios of PtZn-1 are given in Table 1. In comparison to pure Pt and pure Zn [23], the Pt $4f_{7/2}$ and Zn $2p_{1/2}$ binding energies in PtZn-1 film (100 s) increase 0.1 eV and decrease 0.5 eV, respectively. For PtZn-1 (1000 s), the two binding energies increase 0.2 eV and decrease 0.4 eV, respectively. Here, we can conclude that the formation of Pt–Zn bonds increases the binding energy of the core level of Pt, and reduces the binding energy of the core level of Zn [24]. Prolonging the cathodic polarization time from 100 s to 1000 s, the Zn content in the PtZn-1 alloy surface increased from 28.5 to 32.8 at.%, and the latter Zn content was consistent with that of the cover layer measured by EDS (Fig. 3(a)).

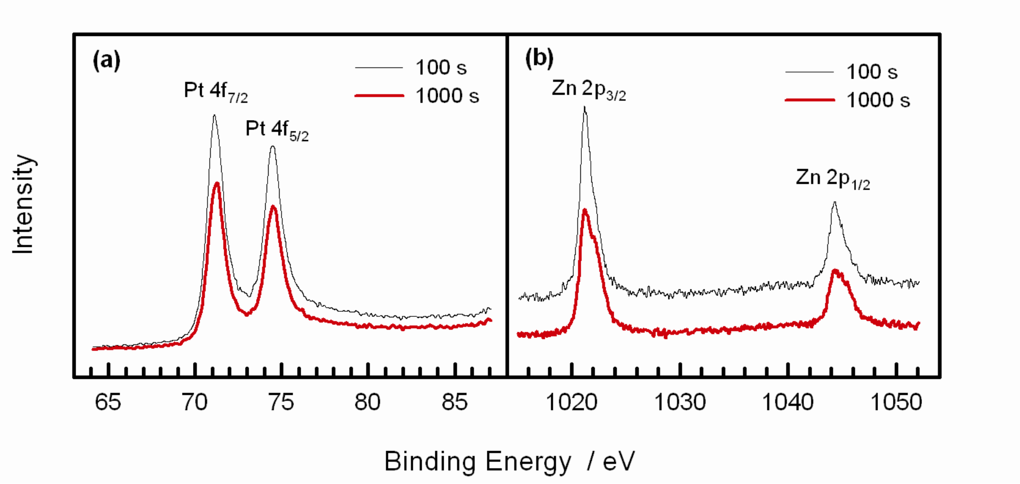

Figure 4. XPS spectra for the hierarchical PtZn-1 alloy films obtained under –6 V for 100 s and 1000 s. (a) Pt 4f and (b) Zn 2p.

Table 1. Binding energies and Pt:Zn atomic ratios for PtZn-1 films.

Sample	Pt 4 $f_{7/2}$ (eV)	Zn $2p_{1/2}$ (eV)	Pt:Zn atomic ratio
PtZn alloy (100 s)	71.1	1044.3	71.5:28.5
PtZn alloy (1000 s)	71.2	1044.4	67.2:32.8
Pt reference [23]	71.0	-	-
Zn reference [23]	-	1044.8	-

Under highly cathodic polarization, several processes could happen on the Pt electrode in the NaOH solution containing low concentration of $ZnSO_4$. (i) Dentritic Zn grew onto the Pt substrate rapidly and a thin PtZn alloy film formed between the deposited Zn and the Pt substrate due to fast diffusion of Zn into Pt [18]. (ii) Hydrogen evolution also occurred concomitantly, and the formation, growth, merging and departure of bubbles may produce strong impact force to accelerate the mutual diffusion of Zn and Pt and thus their alloying process. This effect is similar to mechanical alloying [25]. Moreover, the PtZn film became fractured, wrinkled and curly under the vigorous hydrogen release, resulting in a high rough surface. (iii) At quite negative potentials, the formation/decomposition of surface Zintl compound of Pt would cause the Pt surface roughing [26]. Such a rough surface owns much higher surface energy than a smooth one and would alloy with the electrodeposited Zn more easily. (iv) At the same time, most of soluble Zn source near the electrode surface was consumed by electrodeposition in process (i) and thus a competitive process of cathodic corrosion of Pt happened under the cracks easily in the alkaline solution [27], resulting in nanoporous structures. Besides, other processes such as spontaneous chemical dissolution of bulk and alloyed Zn [28] and hydrogen permeation [29] could also occur. These interface processes give rise to the rough and hierarchical surface.

The electrocatalytic activities towards the oxidation of formic acid and methanol on the PtZn-1, PtZn-2, PtZn-3 and smooth Pt electrodes are exhibited in Fig. 5. Markedly negative shift (at least 70 mV) in the onset potential occurs on the PtZn-1 film for the oxidation of formic acid compared to the other three electrodes (Fig. 5a), and the normalized catalytic current density at –0.1 V on the PtZn-1 film (1000 s) is about 1.8, 3.3 and 9.5 times as larger as that on the PtZn-3, PtZn-2 and smooth Pt electrodes, respectively (Fig. 5b). In addition, the current density in Fig. 5b (the solid line) rises firstly and then reaches to the maximum (1.54 $mA{\cdot}cm^{-2}$) by prolonging the cathodic polarization time during PtZn preparation. As shown in Fig. 5(c-d), the PtZn-1 film also exhibits a better electrocatalytic activity (negative shift in the onset potential and enhanced oxidation current) towards to the oxidation of methanol. The current density on PtZn-1 prepared for 2000 s is 1.38 $mA{\cdot}cm^{-2}$ at 0.1 V, which is 2.9, 2.2, 11 times as larger as that on the PtZn-3, PtZn-2 and smooth Pt electrodes, respectively (Fig. 5d). Meanwhile, as the cathodic polarization time increases, the catalytic current on the PtZn-1 film goes up and then keeps stable (Fig. 5d).

In addition to the high surface area of the hierarchical structure, the enhanced electrocatalytic activities for PtZn-1 films should also be ascribed to the key role of Zn. The Zn component in PtZn alloy could effectively suppress the decomposition of formic acid to poisonous CO_{ad} because of the “third body” effect [30]. So the electrooxidation of formic acid proceeds mainly via the path of active intermediates. Meanwhile, there are a large number of PtZn pairs in PtZn films. Hydroxyl (-OH) can easily form on the Zn component as Zn-OH which would react with the adsorbed carbon monoxide on neighbor Pt sites (Pt-CO) from the dissociation of methanol. Therefore, the poisonous CO intermediate could be effectively removed on the PtZn alloy films by the synergistic reaction [31]. Besides, as shown by the XPS analysis, the Zn atoms can modify the electronic structure of nearby Pt atoms, which is beneficial to the electrooxidation of formic acid and methanol through weakening the CO adsorption on Pt [31, 32].

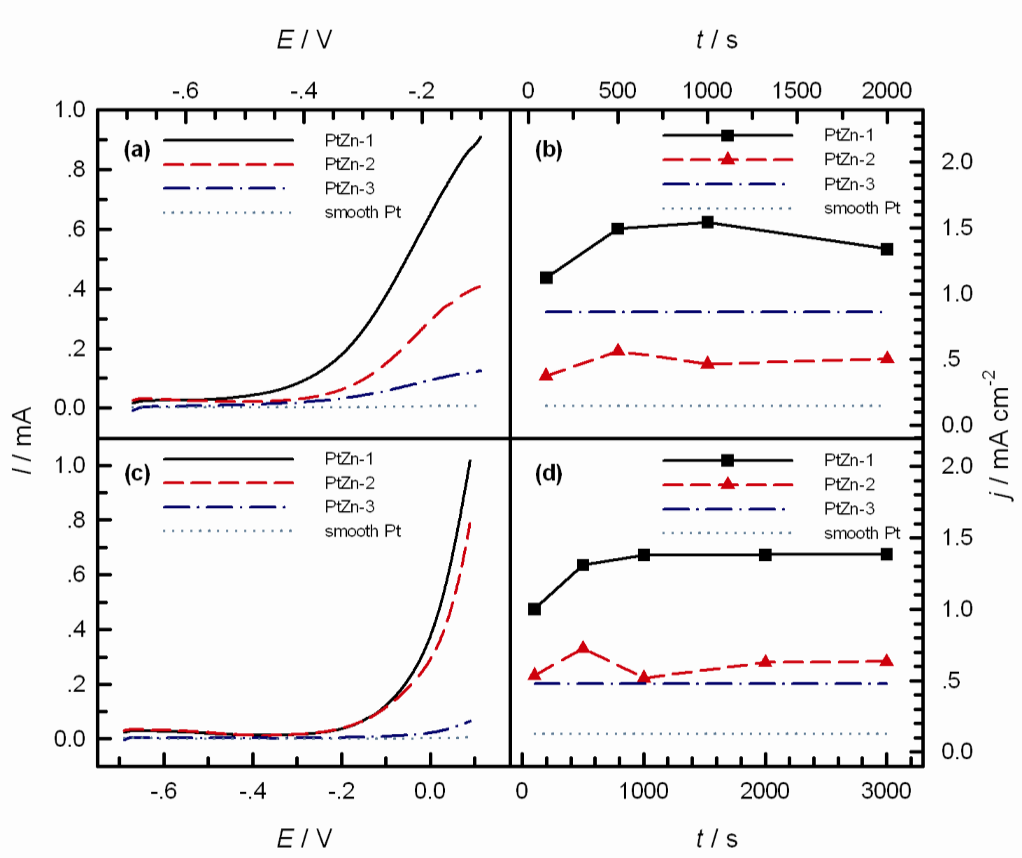

Figure 5. (a, c) Voltammograms at 0.1 V s^{-1} and (b, d) catalytic current density-cathodic polarization time curves on PtZn and smooth Pt electrodes in (a, b) 0.5 mol/L H_2SO_4 + 0.5 mol/L HCOOH and (c, d) 0.5 mol/L H_2SO_4 + 0.5 mol/L CH_3OH. The vertical coordinates in (a) and (c) show the actual currents. The current densities in (b) and (d) are collected from corresponding CV data at the potential of (b) –0.1 V and (d) 0.1 V, respectively. The data on PtZn-3 film (the dotted-dashed lines) and smooth Pt (the dotted lines) electrodes are also given for comparison.

4. CONCLUSIONS

In summary, hierarchically PtZn alloy films were fabricated from a smooth Pt substrate under highly cathodic polarization in an alkaline aqueous solution of low concentration of $ZnSO_4$ at a moderate temperature of 40 °C. Several interfacial processes, such as electrodeposition and alloying of Zn, hydrogen evolution, cathodic corrosion of Pt, were responsible for the formation of such structure. The as-prepared PtZn alloy films exhibited high electrocatalytic activities toward the oxidation of methanol and formic acid comparing to the smooth Pt and the PtZn films prepared under less cathodic polarization (without hydrogen evolution). We expect that this alloying method under highly cathodic polarization can be extended to the non-Zn and/or non-Pt alloy systems.

ACKNOWLEDGEMENTS

We are grateful for the financial supports of this research from National Natural Science Foundation of China (Grant Nos. 21173075 and 21003045), Ph. D. Programs Foundation of the Education Ministry of China (Grant No. 20104306110003).

References

1. R. Parsons and T. VanderNoot, *J. Electroanal. Chem.*, 257 (1988) 9.
1. P. Costamagna and S. Srinivasan, *J. Power Sources*, 102 (2001) 242
2. C. X. Xu, R. Y. Wang, M. W. Chen, Y. Zhang and Y. Ding, *Phys. Chem. Chem. Phys.*, 12 (2010) 239.
3. C. X. Xu, L. Wang, X. L. Mu and Y. Ding, *Langmuir*, 26 (2010) 7437.
4. S. M. Hwang, J. E. Bonevich, J. J. Kim and T. P. Moffat, *J. Electrochem. Soc.*, 158 (2011) B1019 .
5. R. T. S. Oliveira, M. C. Santos, P. A. P. Nascente, L. O. S Bulhões and E. C. Pereira, *Int. J. Electrochem. Sci.*, 3 (2008) 970.
6. L. F. Liu, E. Pippel, R. Scholz and U. Gösele, *Nano. Lett.*, 9 (2009) 4352.
7. C. X. Xu, L. Q. Wang, R. Y. Wang, K. Wang, Y. Zhang, F. Tian and Y. Ding, *Adv. Mater.*, 21 (2009) 2165.
8. Z. F. Liu, J. E. Hu, Q. Wang, K. Gaskell, A. I. Frenkel, G. S. Jackson and B. Eichhorn, *J. Am. Chem. Soc.*, 131 (2009) 6924.
9. S. J. Jiang, Y. W. Ma, H. S. Tao, G. Q. Jian, X. Z. Wang, Y. N. Fan, J. M. Zhu and Z. Hu, *J. Nanosci. Nanotechnol.*, 10 (2010) 3895.
10. Z. F. Liu, D. Reed, G. Kwon, M. Shamsuzzoha and D. E. Nikles, *J. Phys. Chem. C*, 111 (200**7)** 14223.
11. J. A. Rodriguez and M. Kuhn, *J. Phys. Chem.*, 100 (1996) 381.
12. A. Miura, H. S. Wang, B. M. Leonard, H. D. Abruña and F. J. DiSalvo, *Chem. Mater.*, 21 (2009) 2661.
13. J. F. Huang and I. W. Sun, *Chem. Mater.*, 16 (2004) 1829.
14. J. F. Huang and I. W. Sun, *Electrochim. Acta*, 49 (2004) 3251.
15. A. Sode, A. Musgrove and D. Bizzotto, *J. Phys. Chem. C*, 114 (2010) 546.
16. A. Sode, W. Li, Y. G. Yang, P. C. Wong, E. Gyenge, K. A. R. Mitchell and D. Bizzotto, *J. Phys. Chem. B*, 110 (2006) 8715.
17. H. H. Uhlig, J. S. MacNairn and D. A. Vaughn, *Acta Metall.*, 3 (1955) 302.
18. T. Biegler, D. A. J. Rand and R. Woods, *J. Electroanal. Chem.*, 29 (1971) 269.
19. E. Guerra, G. H. Kelsall, M. Bestetti, D. Dreisinger, K. Wong, K. A. R. Mitchell and D. Bizzotto, *J. Electrochem. Soc.*, 151 (2004) E1.
20. T. Boiadjieva, M. Monev, A. Tomandl, H. Kronberger and G. Fafilek, *J. Solid State Electrochem.*, 13 (2009) 671.
21. Zs. Kasztovszky, E. Panczyk, W. Fedorowicz, Zs. Révay and B. Sartowska, *J. Radioanal. Nucl. Chem.*, 265 (2005) 193.
22. B. V. Crist, *Handbook of Monochromatic XPS Spectra*, Chichester/New York (2000).
23. J. A. Rodriguez and M. Kuhn, *J. Chem. Phys.*, 102 (1995) 4279.
24. C. Suryanarayana, *Prog. Mater. Sci.*, 46 (2001) 1.
25. J. Simonet, *Platinum Metals Rev.*, 50 (2006) 180.

26. A. I. Yanson, P. Rodriguez, N. Garcia-Araez, R. V. Mom, F. D. Tichelaar and M. T. M. Koper, *Angew Chem. Int. Ed.*, 50 (2011) 1.
27. S. Sattayasamitsathit, P. Thavarungkul, C. Thammakhet, W. Limbut, A. Numnuam, C. Buranachai and P. Kanatharana, *Electroanalysis*, 21 (2009) 2371.
28. J. O’M. Bockris, M. A. Genshaw and M. Fullenwider, *Electrochim. Acta*, 15 (1970) 47.
29. H. Angerstein-Kozlowska, B. MacDougall and B. E. Conway, *J. Electrochem. Soc.*, 20 (1973) 756.
30. J. S. Spendelow, P. K. Babu and A. Wieckowski. *Curr. Opin. Solid State Mater. Sci.*, 9 (2005) 37.
31. J. Liu, L. Cao, W. Huang and Z. L. Li, *ACS Appl. Mater. Interfaces*, 3 (2011) 3552.